Title	Ascorbate-enabled C-H bond amination catalyzed by myoglobin reconstituted with a trifluoromethyl-substituted Iron porphyrin
Author(s)	Sonoda, Chihiro; Hayashi, Takashi
Citation	Journal of Inorganic Biochemistry. 2026, 277, p. 113207
Version Type	VoR
URL	https://hdl.handle.net/11094/104035
rights	This article is licensed under a Creative Commons Attribution-NonCommercial 4.0 International License.
Note	

Journal of Inorganic Biochemistry 277 (2026) 113207

Contents lists available at ScienceDirect

Journal of Inorganic Biochemistry

journal homepage: www.elsevier.com/locate/jinorgbio

Ascorbate-enabled C-H bond amination catalyzed by myoglobin reconstituted with a trifluoromethyl-substituted Iron porphyrin☆

Chihiro Sonoda, Takashi Hayashi *

Department of Applied Chemistry, Graduate School of Engineering, The University of Osaka, Suita, Osaka 565-0871, Japan

ARTICLE INFO

Keywords:
Hemoprotein
Artificial metalloenzyme
Nitrene transfer
Reconstituted myoglobin
Sultam synthesis
CF_3 iron porphyrin

ABSTRACT

Nitrogen-containing organic molecules are essential structural motifs in bioactive compounds, pharmaceuticals and functional materials. Direct C-H amination via nitrene transfer provides an efficient and atom-economical route for C-N bond formation. However, most hemoprotein-based catalysts require strong reductants such as dithionite to generate the metal–nitrene intermediate. Here, we report myoglobin reconstituted with an iron complex ($FePor(CF_3)_2$) bearing two trifluoromethyl groups at the pyrrole β-positions of the porphyrin framework. This arrangement promotes intramolecular benzylic C-H bond amination under mild conditions using sodium L-ascorbate as the sole reductant. The $FePor(CF_3)_2$ cofactor exhibits a positively shifted Fe(III)/Fe(II) redox potential that allows efficient reduction to occur in the protein scaffold and suppresses noncatalytic substrate reduction, leading to improved chemoselectivity for secondary C-H bond amination. The H64A mutant of myoglobin reconstituted with $FePor(CF_3)_2$ achieved a turnover number (TON) of 133 for tertiary benzylic C-H amination. Kinetic studies revealed that the reaction rate is inversely correlated with the C-H bond dissociation energy, with a smaller negative slope in the bond dissociation energies (BDEs) plot compared to a synthetic cofactor with a negative redox potential. This suggests that there is a mechanistic shift in the rate-determining step from hydrogen atom transfer to nitrene formation. These findings highlight the potential of cofactor redox tuning to control reactivity and selectivity in artificial heme enzymes for abiological C-H bond functionalization.

1. Introduction

Amines are important structural motifs in biologically active natural products, pharmaceuticals and functional materials [1] because the incorporation of nitrogen-containing groups into organic compounds often leads to significant changes in their physicochemical properties and biological activities [2–4]. Conventional synthetic approaches to access amines, such as nucleophilic substitution [5,6], reductive amination [7] and metal-catalyzed C-N coupling reactions [8], are well established. However, these strategies typically rely on pre-functionalized substrates, resulting in low atom economy and are potentially unsuitable for late-stage functionalization of complex molecules [9]. Therefore, direct C-H functionalization has emerged as a powerful approach to improve atom and step economy. In particular, C(sp^3)–H bond amination, which directly converts normally inert C-H bonds into C-N bonds without prior activation, is highly attractive for development [10].

On the other hand, transaminase-mediated biocatalytic processes can selectively introduce free amines but require pre-oxidized substrates and do not directly operate on C-H bonds [11–13]. Over the past few decades, transition metal-catalyzed nitrene transfer reactions have been widely investigated as an efficient strategy for C-N bond formation at C-H sites. Catalytic systems employing rhodium, iridium, ruthenium, iron and silver complexes, are frequently combined with nitrene precursors such as iminoiodinanes or sulfonyl azides, demonstrating high reactivity and expanding the scope of potential substrates [14–18]. However, despite significant advances in chemical toolsets and enantioselective variants, there are no known examples of a natural enzyme directly mediating nitrene insertion into saturated C-H bonds. The development of an enzymatic platform to enable such transformations would represent a major advance toward the sustainable and environmentally friendly synthesis of nitrogen-containing molecules [19].

In nature, cytochrome P450 monooxygenases selectively oxidize C-H bonds through the generation of a high-valent iron–oxo intermediate species of the heme cofactor, which is known as Compound I. The close similarity between this reactive species and the metal–nitrene

---

☆ This article is part of a Special issue entitled: 'CanBic9' published in Journal of Inorganic Biochemistry.

* Corresponding author.

E-mail address: thayashi@chem.eng.osaka-u.ac.jp (T. Hayashi).

https://doi.org/10.1016/j.jinorgbio.2025.113207
Received 30 November 2025; Received in revised form 22 December 2025; Accepted 27 December 2025

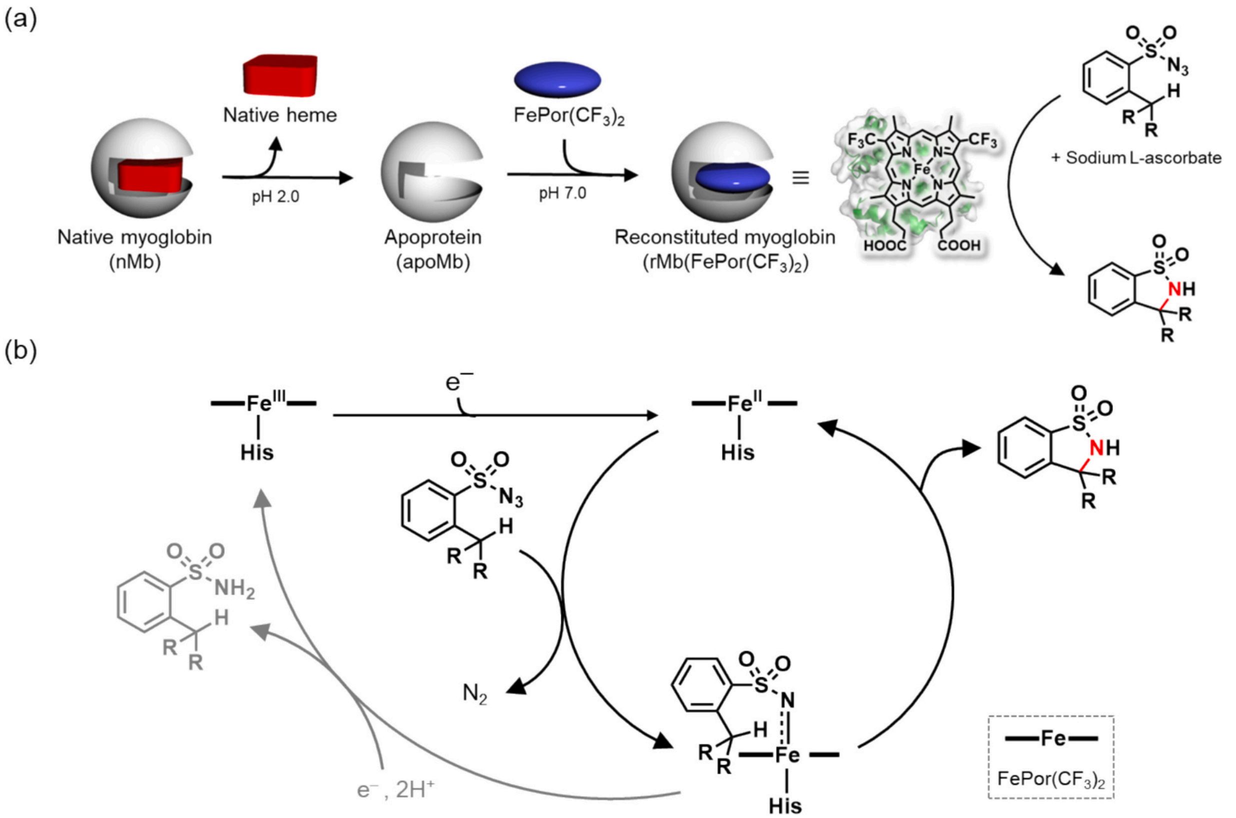

Fig. 1. (a) Intramolecular C-H bond amination of arylsulfonyl azides catalyzed rMb(FePor(CF₃)₂) under remarkably mild conditions. (b) Plausible reaction mechanism of C-H bond amination. Substituent moieties that are not involved in the reaction mechanism are omitted.

intermediates involved in C-H amination has motivated the design of biomimetic catalysts using synthetic metalloporphyrinoids [20–22]. Metalloporphyrin cofactors can be tuned by varying either the metal center and/or the substituents of the porphyrin macrocycle to modulate redox potential and reactivity and enable rational design of catalysts with desired chemical functions. In parallel, *heme enzyme engineering* has been actively pursued to endow natural biological scaffolds with new reactivities and selectivities. In early studies, cytochrome P450 was reported to mediate C-H amination reactions using *N*-tosyliminoaryliodinane as a nitrene donor [23]. Subsequently, a series of P450 variants known as P411s, in which the axial cysteine ligand was replaced with serine, were found to yield highly active and enantioselective nitrene transferases capable of catalyzing C-H amination, aziridination and sulfimidation [24–31]. This field has been further expanded by developing both P450 and myoglobin variants that promote intra- and intermolecular C-H amination of sulfonyl azides, highlighting the ability of hemoprotein scaffolds to support abiological nitrene chemistry [32–36].

While mutagenesis and directed evolution have proven effective, *cofactor replacement* offers a complementary approach for tuning reactivity. Hartwig and co-workers demonstrated that replacing the heme iron center with iridium in the thermophilic enzyme CYP119 from *Sulfolobus solfataricus* generates a hybrid Ir–heme enzyme capable of promoting C-H amination [37]. Moreover, studies on synthetic metalloporphyrins have shown that modifying the porphyrin frameworks can significantly alter reactivity and selectivity [38–40]. Despite these findings, examples of nitrene transfer using artificial porphyrinoids embedded within protein matrices remain limited. Our research group has systematically explored hemoproteins reconstituted with synthetic metalloporphyrinoids as artificial metalloenzymes with tailored redox and electronic properties [41–48]. In particular, metal complexes of porphycene, a constitutional isomer of porphyrin, have revealed distinctive reactivities when incorporated into myoglobin, supporting reactions such as peroxidation, hydroxylation and carbene transfer [44–48]. We recently showed that myoglobin containing iron porphycene (rMb(FePc)) catalyzes intramolecular C-H bond amination of arylsulfonyl azides to form sultam products with exceptional turnover numbers exceeding 10^4, indicating significantly greater activity than native myoglobin (nMb) [47]. The enhancement was attributed to the efficient formation of a high-valent Fe–nitrene intermediate within the porphycene framework. However, this system still requires a strong chemical reductant such as sodium dithionite and exhibits side reactions associated with undesirable nitrene reduction and non-catalytic reduction.

To overcome these limitations, we focused on redox engineering of the cofactor framework. In our previous study, we reported that reconstitution of myoglobin with an iron complex FePor(CF₃)₂, porphyrin with two trifluoromethyl group substituted at the pyrrole β-positions, results in a positive shift in the Fe(III)/Fe(II) redox potential, enhancing the reactivity of the corresponding carbene intermediates in alkene cyclopropanation [48]. Furthermore, we previously found that FePor(CF₃)₂ promotes the cyclopropanation reaction within the apomyoglobin matrix even in the absence of dithionite. These results suggest that increasing the electron-withdrawing nature of the ligand of the cofactor can facilitate the formation of reactive low-valent species under milder reducing conditions.

In this study, we extend this concept to nitrene chemistry and demonstrate that myoglobin reconstituted with FePor(CF₃)₂, (herein designated rMb(FePor(CF₃)₂)), catalyzes intramolecular C-H bond amination of arylsulfonyl azides under mild conditions (Fig. 1). The positively shifted redox potential of FePor(CF₃)₂ provides efficient reduction of the ferric enzyme using weak reductants such as sodium L-ascorbate, eliminating the need for dithionite. Moreover, the electron-deficient cofactor promotes the C-H bond amination, improving chemoselectivity for C-N bond formation against simple substrate reduction. This study demonstrates that fine-tuning the redox landscape of the heme analog through cofactor modification provides an effective strategy for designing artificial metalloenzymes capable of performing abiological C-H functionalization reactions.

2. Experimental procedures

2.1. Instruments

UV–Vis absorption spectra were recorded using a UV-2700 or UV-3600 double-beam spectrophotometer (Shimadzu), and in some cases a BioSpec-nano spectrometer (Shimadzu). The pH of each solution was measured with an F-72 pH meter (Horiba). Electrospray ionization time-of-flight mass spectra (ESI-TOF MS) were measured with a compact ESI-QTOF mass spectrometer (Bruker). High-performance liquid chromatography (HPLC) analyses were carried out on Shimadzu HPLC systems (20AD or 40AD) equipped with a YMC-Triart C18 column (YMC; 5 μm, 4.6 mm × 150 mm) or a CHIRALPAK® IA-3 column (DAICEL; 3 μm, 4.6 mm × 250 mm). All air-sensitive operations were performed under an inert atmosphere using a UNILab glove box (MBRAUN). Transient UV–Vis measurements were performed using a rapid scan stopped-flow system (Unisoku) constructed with a Xe light source. Electrochemical studies were carried out using a potentiostat (CompactStat, Ivium Technologies) with a Pt mesh working electrode, a Pt wire counter electrode and an Ag|AgCl reference electrode (3 M $NaCl_{aq}$, BAS) under anaerobic conditions.

2.2. Materials

All chemicals were purchased from FUJIFILM Wako, TCI, Sigma-Aldrich and Nacalai Tesque, and were used without further purification unless otherwise noted. Distilled water was demineralized using a Millipore Integral 3. Horse heart Mb was purchased from Sigma-Aldrich and purified by CM-Cellulose cation exchange column (FUJIFILM Wako). Glucose oxidase was purchased from FUJIFILM Wako and catalase from bovine liver was purchased from TCI. The myoglobin variant was recombinantly expressed and purified according to our previous reports with several modifications [48]. Removal of heme from native myoglobin (nMb) and its H64A variant (Mb^{H64A}) and preparation of reconstituted proteins with $FePor(CF_3)_2$, $rMb(FePor(CF_3)_2)$ and $rMb^{H64A}(FePor(CF_3)_2)$, were performed according to procedures also described in a previous report [48]. Arylsulfonyl azide substrates and authentic samples of corresponding sultam analogues and sulfonamide were prepared as reported [32].

Table 1
C–H bond amination of 2,4,6-triethylbenzenesulfonyl azide (**1**) in the presence of dithionite[a].

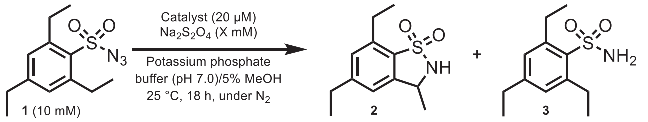

Entry	Catalyst	$Na_2S_2O_4$ concentration	TON(**2**)	TON(**3**)	**2: 3**
1	$rMb(FePor(CF_3)_2)$	0.1 mM	0.8	1.4	38:62
2	$rMb(FePor(CF_3)_2)$	1 mM	9.3	29.7	24:76
3	$rMb(FePor(CF_3)_2)$	10 mM	5.1	85.4	5:95
4	nMb	0.1 mM	0.3	0.8	29:71
5	nMb	1 mM	2.8	36.3	7:93
6	nMb	10 mM	1.8	88.9	2:98

[a] Conditions: [catalyst] = 20 μM, [$Na_2S_2O_4$] = 0.1, 1 or 10 mM, [substrate] = 10 mM in 100 mM potassium phosphate buffer (pH 7.0) containing 5 % MeOH at 25 °C for 18 h under a N_2 atmosphere.

2.3. General procedures for intramolecular C – H bond amination

The reactions were performed in a total volume of 500 μL of 100 mM potassium phosphate buffer (pH 7.0) containing 5 % methanol at 25 °C for 18 h. The buffer solution containing the protein (23.2 μM, 430 μL) and a GOx solution (10 μL of a stock solution containing ca. 35,000 $U\cdot mL^{-1}$ catalase and ca. 2500 $U\cdot mL^{-1}$ glucose oxidase in KPi buffer) was gently degassed in a chamber of a glove box. After placing this mixture into the glove box, a 1250 mM D-glucose aqueous solution (10 μL) and 20 mM sodium L-ascorbate aqueous solution (25 μL) was added. After incubation for 10 min at 25 °C to ensure complete reduction of the protein, the reaction was initiated by adding 25 μL of a 200 mM substrate solution in methanol.

After the reaction was complete, 10 μL of 50 mM benzyl alcohol in acetonitrile was added as an internal standard. Subsequently, the reaction mixture was extracted with 500 μL of diethyl ether by vigorous vortex mixing to recover the organic components. The resulting organic phase was separated and concentrated under a gentle N_2 stream, and the residue was redissolved in 200 μL methanol. The obtained solution was subjected to HPLC analysis. Detailed analytical conditions are shown in Table S1. The reaction products were identified by comparing their retention times with those of authentic standards analyzed under identical conditions.

2.4. Kinetic studies

To evaluate the relationship between C-H bond strength and reaction rate, a bond dissociation energy (BDE) plot was constructed. The reactions were carried out according to the general procedure using 20 μM catalyst, 10 mM sodium L-ascorbate and 10 mM substrate under the standard conditions. After 18 h of incubation, the reaction was quenched, and the resulting mixtures were analyzed to determine the rate of the C-H bond amination for use in the BDE correlation.

2.5. Spectroelectrochemical measurements of the proteins

Spectroelectrochemical measurements were carried out at 25 °C using an optically transparent thin-layer electrode cell (optical pathlength of 1 mm) under a N_2 atmosphere with a Pt mesh working electrode, a Pt wire counter electrode, and an Ag|AgCl reference electrode (3 M $NaCl_{aq}$, BAS). The potentials of these electrodes were controlled and measured with a potentiostat (CompactStat, Ivium Technologies). A solution of Mb^{H64A} with GOx solution and Fe(III)-EDTA (500 μM), 2,3,5,6-tetramethylphenylenediamine (20 μM), 2-hydroxy-1,4-naphthoquinone (20 μM) and $Ru(NH_3)_6Cl_3$ (100 μM) as electron mediators was prepared in 100 mM potassium phosphate buffer (pH 7.0). A solution of $rMb^{H64A}(FePor(CF_3)_2)$ with GOx solution and Fe(III)-EDTA (500 μM), 2,3,5,6-tetramethylphenylenediamine (500 μM) and potassium hexacyanidoferrate(III) (500 μM) as electron mediators was prepared in 100 mM potassium phosphate buffer (pH 7.0). At each applied potential, the electronic absorption spectra were monitored after a point in time when no further current changes were detected. The plots were fitted to the Nernst equation and the number of electrons related to the reaction was determined through a slope of its fitting curve.

2.6. Reduction of the proteins by sodium L-ascorbate

2.6.1. UV–Vis absorption spectra

The buffer solution containing the protein (23.2 μM, 215 μL) and a GOx solution (5 μL of stock solution containing ca. 35,000 $U\cdot mL^{-1}$ catalase and ca. 2500 $U\cdot mL^{-1}$ glucose oxidase in KPi buffer) was gently degassed in a chamber of a glove box. After placing this mixture into a glove box, a 1250 mM D-glucose aqueous solution (5 μL) was added. After removal from the glove box, a degassed solution of 20 mM sodium L-ascorbate aqueous solution (12.5 μL) was added and UV–Vis spectral changes were recorded.

Table 2
C–H bond amination of 2,4,6-triethylbenzenesulfonyl azide (**1**) in the presence of sodium L-ascorbate[a].

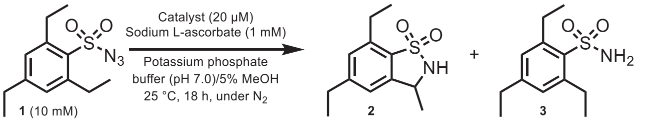

Entry	Catalyst	TON(**2**)	**2**: **3**
1	rMb(FePor(CF_3)$_2$)	0.6	47:53
2	nMb	0.4	39:61
3	Mb^{H64A}	9.0	72:28
4	rMb^{H64A}(FePor(CF_3)$_2$)	17.4	76:24
5	rMb^{H64A}(FePor(CF_3)$_2$)[b]	42.3	67:33
6	rMb^{H64A}(FePor(CF_3)$_2$)[c]	48.3	26:74

[a] Conditions: [catalyst] = 20 μM, [sodium L-ascorbate] = 1 mM, [substrate] = 10 mM in 100 mM potassium phosphate buffer (pH 7.0) containing 5 % MeOH at 25 °C for 18 h under a N_2 atmosphere. [b][sodium L-ascorbate] = 10 mM. [c]using 10 mM dithionite instead of sodium L-ascorbate.

2.6.2. *Stopped-flow single mixing analysis*

To a solution of rMb^{H64A}(FePor(CF_3)$_2$) (22 μM, 250 μL) in 100 mM potassium phosphate buffer at pH 7.0, a 2.0 mM sodium L-ascorbate aqueous solution (250 μL) in 100 mM potassium phosphate buffer at pH 7.0 was added under an N_2 atmosphere and UV–Vis spectral changes were recorded.

3. Results and discussion

3.1. *Intramolecular C-H bond amination by rMb(FePor(CF_3)$_2$)*

In our preliminary experiments, we examined the intramolecular C-H bond amination of 2,4,6-triethylbenzenesulfonyl azide (**1**) catalyzed by horse heart myoglobin reconstituted with FePor(CF_3)$_2$ (rMb(FePor(CF_3)$_2$)) under reducing conditions. The reaction afforded 5,7-diethyl-3-methyl-2,3-dihydrobenzo[*d*]isothiazole-1,1-dioxide (**2**) as a sultam analogue, accompanied by the formation of sulfonamide **3** as a byproduct arising from azide reduction. Table 1 summarizes the product yields, turnover numbers (TONs), and product/byproduct ratios obtained under N_2 atmosphere with 0.2 mol% catalyst in the presence of dithionite. The TON and the selectivity for products **2** and **3** were found to depend on the concentration of dithionite. The highest TON (9.3) was obtained at a dithionite concentration of 1 mM, while the highest selectivity for **2** (ratio of **2** relative to the sum of **2** and **3**: 38 %) was observed at a dithionite concentration of 0.1 mM. At higher concentrations (10 mM), the noncatalytic reduction of the azide substrate by dithionite competes with the catalytic reaction, significantly decreasing the selectivity and the TON for **2**. Under all conditions examined, rMb (FePor(CF_3)$_2$) exhibits a higher TON than native myoglobin. Because the noncatalytic substrate reduction occurs at all dithionite concentrations, the reaction was next tested using sodium L-ascorbate (1 mM), a milder reductant (Table 2). In this case, noncatalytic reduction is suppressed, but only trace amounts of product were detected for both nMb and rMb (FePor(CF_3)$_2$). To improve catalytic turnover, the H64A variant, in which the distal histidine (His64) was replaced with alanine to facilitate substrate access to the active site, was evaluated as the protein scaffold. The native heme-containing variant, Mb^{H64A}, exhibits a TON of 9.0 for the formation of **2**, whereas reconstitution with FePor(CF_3)$_2$ significantly improves the TON to 17.4, which further increases to 42.3 under optimized conditions. The selectivity toward **2** is also significantly enhanced compared to reactions using dithionite as the reductant. When rMb^{H64A}(FePor(CF_3)$_2$) is used as the catalyst with 1 mM sodium L-ascorbate, the selectivity reaches 76 %. Since noncatalytic azide reduction is largely suppressed under these conditions, the formation of sulfonamide **3** is likely to arise from further reduction of an intermediate. When the concentration of sodium L-ascorbate is increased to 10 mM, this reduction process becomes more pronounced, resulting in a slight decrease in selectivity (67 %). Under otherwise identical conditions, using 10 mM dithionite instead of sodium L-ascorbate with rMb^{H64A}(FePor(CF_3)$_2$) results in a TON of 48.3, which is similar to that of **2** using 10 mM ascorbate, but with a significantly reduced selectivity of 26 %. When 2,4,6-triisopropylbenzenesulfonyl azide (**4**) is used as the substrate, the reaction proceeds more efficiently to afford 5,7-diisopropyl-3,3-dimethyl-2,3-dihydrobenzo[*d*]isothiazole-1,1-dioxide (**5**) with a remarkably high TON of 133 (Table 3). This enhanced TON is attributed to the higher reactivity of tertiary C-H bonds toward amination compared with secondary C-H bonds, consistent with the trend reported in previous studies.

Table 4
Redox potential of myoglobin derivatives[a].

Protein	nMb [49]	Mb^{H64A}	rMb (FePor(CF_3)$_2$) [48]	rMb^{H64A} (FePor(CF_3)$_2$)
Redox potential (vs. NHE)	46 mV	74 mV	147 mV	115 mV

[a] The absorption changes of the proteins obtained from spectroelectrochemical measurements were fitted to Nernst plots.

3.2. *Reduction behaviors of myoglobin and its variants*

Spectroelectrochemical measurements were conducted to determine the redox potentials of the Fe(III)/Fe(II) couple for Mb^{H64A} and rMb^{H64A}(FePor(CF_3)$_2$). The potentials were determined to be 74 mV and 115 mV, respectively. Table 4 summarizes these values in comparison with those of other myoglobin derivatives. The H64A mutation was found to shift the potential to more positive values. The facilitated formation of the ferrous species is consistent with the observation that the catalytic reaction proceeds even with a weak reductant such as sodium L-ascorbate. However, the redox potential of rMb^{H64A}(FePor(CF_3)$_2$) is lower than expected based on its catalytic activity. Although a moderate correlation appears to exist between the redox potential and catalytic

Table 3
C–H bond amination of 2,4,6-triisopropylbenzenesulfonyl azide (**4**)[a].

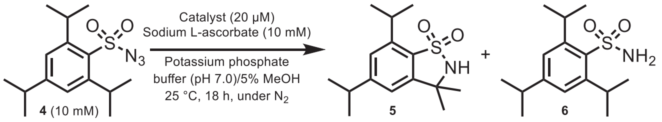

Entry	Catalyst	TON(**5**)	**5**: **6**
1	rMb(FePor(CF_3)$_2$)	11.5	95:5
2	nMb	2.6	82:18
3	rMb^{H64A}(FePor(CF_3)$_2$)	133.0	97:3

[a] Conditions: [catalyst] = 20 μM, [sodium L-ascorbate] = 10 mM, [substrate] = 10 mM in 100 mM potassium phosphate buffer (pH 7.0) containing 5 % MeOH at 25 °C for 18 h under a N_2 atmosphere.

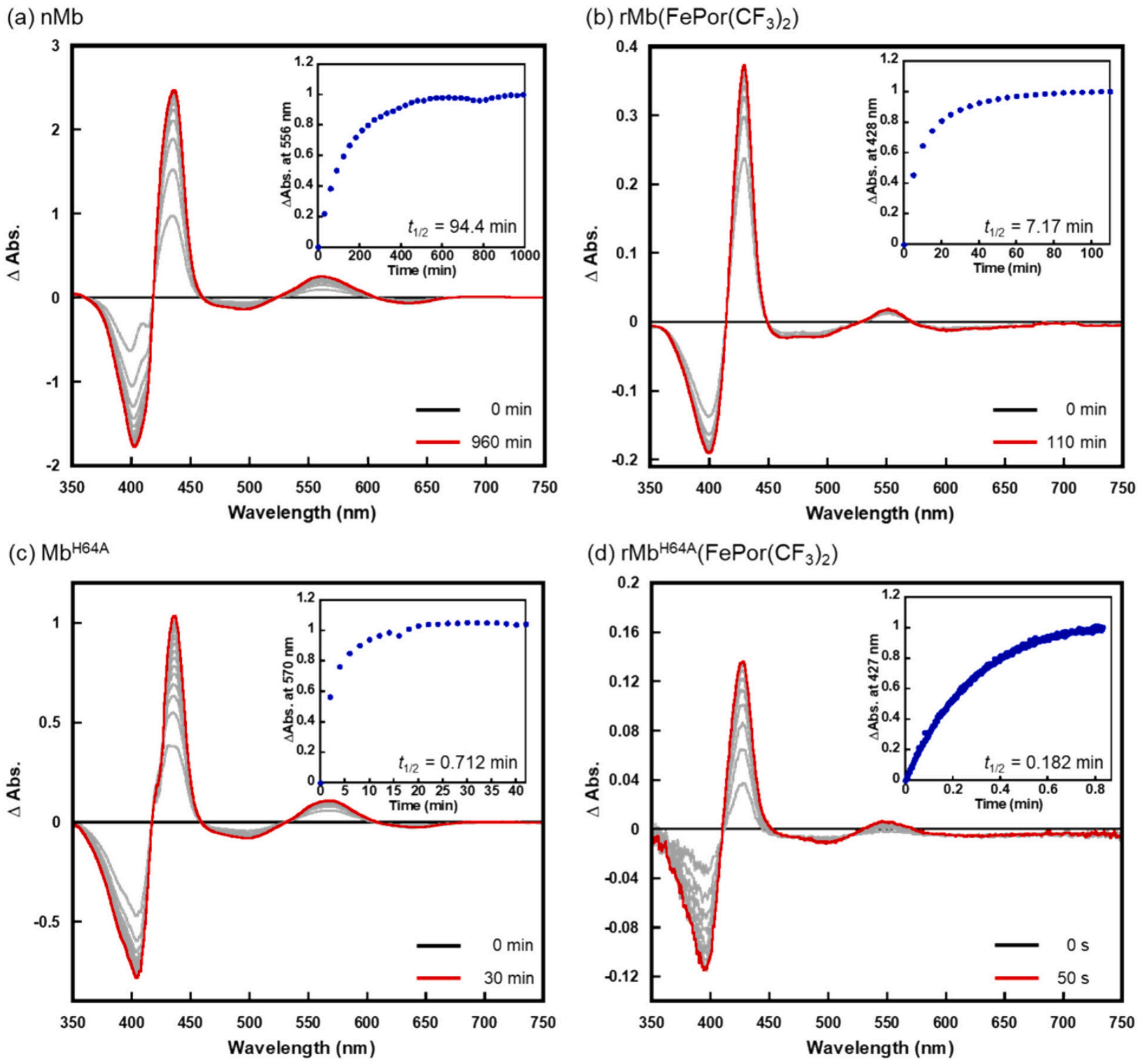

Fig. 2. UV–Vis spectral changes of proteins and time course plots of absorbance changes that occur upon addition of sodium L-ascorbate aqueous solution. (a) UV–Vis spectral changes of nMb monitored at intervals of 60 min. (b) UV–Vis spectral changes of rMb(FePor(CF_3)$_2$) monitored at intervals of 10 min. (c) UV–Vis spectral changes of Mb^{H64A} monitored at intervals of 2 min. (d) UV–Vis spectral change of rMb^{H64A}(FePor(CF_3)$_2$) monitored at intervals of 5 s.

performance, the steric effect of the His64 residue likely exerts a substantial influence that cannot be ignored. The mutation may accelerate access of both sodium L-ascorbate and the substrates to the heme center.

To further examine the accessibility of sodium L-ascorbate to the heme center, the spectral changes which occur upon addition of sodium L-ascorbate were analyzed for each protein sample. Under strict anaerobic conditions with catalase, glucose oxidase and glucose under a N_2 atmosphere, all nMb, rMb(FePor(CF_3)$_2$), Mb^{H64A} and rMb^{H64A}(FePor(CF_3)$_2$) exhibit spectral changes which indicate a transition from the Fe(III) form to the Fe(II) deoxy form with clear isosbestic points (Fig. 2). From these absorbance changes, half-life values of the reactions were determined for each protein. Notably, the reduction rate of rMb^{H64A}(FePor(CF_3)$_2$) was approximately 500 times faster than that of native myoglobin. The half-life value (0.182 min) obtained for rMb^{H64A}(FePor(CF_3)$_2$) is relatively low compared with the reaction time of the catalytic reaction described above, indicating that the reduction proceeds rapidly relative to catalysis. Moreover, the order of the reduction rates correlates well with the trend in TONs observed in the catalytic reactions, suggesting that the improved catalytic efficiency arises not only from differences in redox potential but also from enhanced accessibility of substrates and reductants to the active site.

3.3. Kinetic evaluation of C-H bond amination

Time-course plots of the turnover number (TON) were obtained to determine the reaction rates for the formation of **2** and **5** catalyzed by rMb^{H64A}(FePor(CF_3)$_2$) (Fig. S1). The reactions proceed slowly, and the rates calculated from the slopes are 2.4 h^{-1} for **2** and 7.4 h^{-1} for **5**. In addition, the rate for the reaction of 2,4,6-trimethylbenzenesulfonyl azide (**7**) was determined to be 0.035 h^{-1}. Because the reduction of the ferric enzyme by sodium L-ascorbate is sufficiently rapid, these rate constants are considered to reflect the intrinsic kinetics of nitrene formation and/or C-H bond activation. These kinetic rate constants are lower than that of rMb(FePc) [47], suggesting that in the case of rMb^{H64A}(FePor(CF_3)$_2$), the formation of the nitrene intermediate competes with the hydrogen atom transfer (HAT) step.

The logarithmic values of the observed rate constants (k'_{obs}), normalized by the number of reactive hydrogen atoms, were plotted against the bond dissociation energies (BDEs) of the benzylic C-H bonds of the respective substrates (Fig. 3). A clear negative slope was obtained,

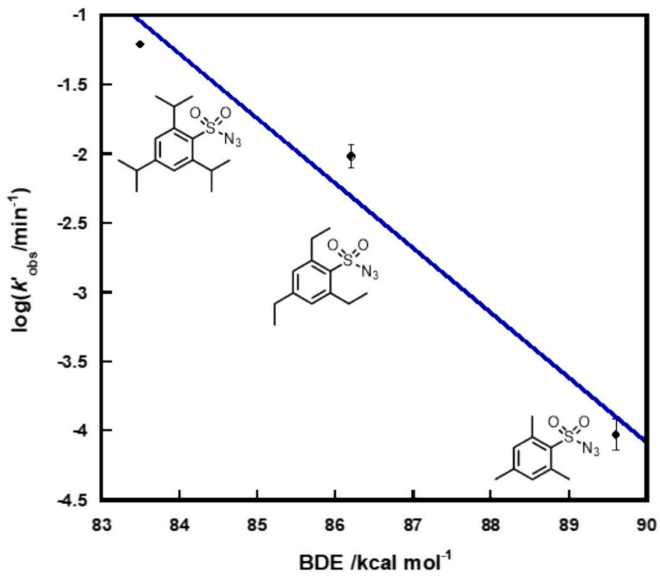

Fig. 3. Plot of $\log(k'_{obs})$ values vs. BDE of C-H bonds for the C−H bond amination of **1**, **4** and **7** catalyzed by $rMb^{H64A}(FePor(CF_3)_2)$.

indicating that the HAT step is involved in the reaction pathway. In the previous study, rMb(FePc) also showed a negative slope. The slope magnitudes obtained from rMb(FePc) and $rMb^{H64A}(FePor(CF_3)_2)$ are −0.59 and −0.47, respectively. Although the numerical difference between the two slopes is not large, this change is reproducible and consistent across all examined data points, indicating a systematic rather than random deviation. Given the typical experimental uncertainties in kinetic measurements of this type, this difference may not be statistically significant in a strict mathematical sense. However, even a modest decrease in the absolute value of the slope can provide mechanistic insights when interpreted within the broader context of these catalytic systems.

Both catalytic systems show a clear negative slope, confirming that the reaction rate decreases with increasing C-H bond dissociation energy and that hydrogen atom transfer (HAT) contributes to the overall rate-determining process. However, the smaller absolute slope observed for $rMb^{H64A}(FePor(CF_3)_2)$ suggests that the reaction rate is less sensitive to the C-H bond strength. This behavior can be rationalized by a change in the rate-determining step. The cofactor FePc, which contains electron-donating ligands, readily accesses the high-valent Fe–nitrene species, making the subsequent C-H bond cleavage and hydrogen atom transfer kinetically dominant. In contrast, the Fe complex of electron-deficient $Por(CF_3)_2$ ligand has a more positive redox potential, suppressing the formation of high-valent intermediates, while the reactivity of the intermediate appears to be high, enabling selective amination of the secondary benzylic C-H bond. Consequently, the formation rate of the nitrene species decreases and begins to limit the overall reaction rate, resulting in observed kinetics showing weaker dependence on the C-H bond strength.

This interpretation is in good agreement with the established redox characteristics of the $FePor(CF_3)_2$ cofactor, which is known to stabilize the ferric resting state and enhance the reactivity of high-valent intermediate. A similar effect was previously observed in our studies of cyclopropanation catalyzed by $rMb^{H64A}(FePor(CF_3)_2)$. Engineered myoglobins with different redox potentials were found to modulate the balance between carbene formation and hydrogen atom transfer. The similarity between the two reactions suggests that the redox tuning of the cofactor by the porphyrinoid framework systematically alters the energetic hierarchy of key reaction steps in the catalysis of nitrene or carbene generation and subsequent substrate activation, thereby determining the kinetic profiles observed in these distinct, yet mechanistically-related transformations.

4. Conclusion

In summary, we found that iron porphyrin with two trifluoromethyl groups in H64A apomyoglobin catalyzes intramolecular benzylic C−H bond amination in the presence of sodium L-ascorbate, a mild reductant. The CF_3-substituted cofactor promotes efficient formation of the ferrous state, as the reducing power of sodium L-ascorbate was sufficient to generate Fe(II) while suppressing noncatalytic reduction of the azide substrate. These results demonstrate that this system is effective for the amination of secondary benzylic C-H bonds. While the catalytic reactivity can be qualitatively rationalized based on the redox potentials of the cofactors, the observed activity also reflects the influence of the protein matrix, where changes in the local environment, including substrate accessibility, cooperatively enhance the catalytic performance. Accumulating such insights into the interplay between cofactor redox properties and protein structure will be crucial for the rational design of next-generation artificial metalloenzymes. Further study is underway to extend this system to other reaction types and protein scaffolds.

CRediT authorship contribution statement

Chihiro Sonoda: Writing – original draft, Investigation. **Takashi Hayashi:** Writing – original draft, Supervision, Conceptualization.

Declaration of competing interest

The authors declare that they have no known competing financial interests or personal relationships that could have appeared to influence the work reported in this paper.

Acknowledgements

This work was supported by Grants-in-Aid for Scientific Research provided by JSPS KAKENHI Grant Number JP25H00887. We appreciate Dr. Koji Oohora (Univ. Osaka) for valuable discussions and support in manuscript preparation.

Appendix A. Supplementary data

Supplementary data to this article can be found online at https://doi.org/10.1016/j.jinorgbio.2025.113207.

References

[1] R. Hili, A.K. Yudin, Making carbon-nitrogen bonds in biological and chemical synthesis, Nat. Chem. Biol. 2 (2006) 284–287, https://doi.org/10.1038/nchembio0606-284.

[2] C.G.L. Veale, Into the fray! A beginner's guide to medicinal chemistry, ChemMedChem 16 (2021) 1199–1225, https://doi.org/10.1002/cmdc.202000929.

[3] M.M. Rezaeifar, A. Abiri, H. Rezaiezadeh, M.R. Tavakoli, M.A. Langarizadeh, Y. Pourshojaei, Phenoxyalkyl cyclic and acyclic amine derivatives: what do they teach us about scaffold-based drug design? Med. Chem. Res. 33 (2024) 703–720, https://doi.org/10.1007/s00044-024-03215-1.

[4] N.S. Troelsen, M.H. Clausen, Library design strategies to accelerate fragment-based drug discovery, Chem. Eur. J. 26 (2020) 11391–11403, https://doi.org/10.1002/chem.202000584.

[5] M. Sánchez-Roselló, M. Escolano, D. Gaviña, C. del Pozo, Two decades of Progress in the asymmetric intramolecular aza-Michael reaction, Chem. Rec. 22 (2022) e202100161, https://doi.org/10.1002/tcr.202100161.

[6] E. Budynina, K. Ivanov, I. Sorokin, M. Melnikov, Ring opening of donor–acceptor cyclopropanes with *N*-nucleophiles, Synthesis 49 (2017) 3035–3068, https://doi.org/10.1055/s-0036-1589021.

[7] O.I. Afanasyev, E. Kuchuk, D.L. Usanov, D. Chusov, Reductive amination in the synthesis of pharmaceuticals, Chem. Rev. 119 (2019) 11857–11911, https://doi.org/10.1021/acs.chemrev.9b00383.

[8] J. Bariwal, E. Van Der Eycken, C–N bond forming cross-coupling reactions: an overview, Chem. Soc. Rev. 42 (2013) 9283–9303, https://doi.org/10.1039/c3cs60228a.

[9] W.-N. Xu, Y.-D. Gao, P. Su, L. Huang, Z.-L. He, L.-C. Yang, Progress in enzyme-catalyzed C(sp^3)–H amination, ACS Catal. 14 (2024) 14139–14160, https://doi.org/10.1021/acscatal.4c04947.

[10] D. Hazelard, P.-A. Nocquet, P. Compain, Catalytic C–H amination at its limits: challenges and solutions, Org. Chem. Front. 4 (2017) 2500–2521, https://doi.org/10.1039/C7QO00547D.

[11] N.J. Turner, Ammonia lyases and aminomutases as biocatalysts for the synthesis of α-amino and β-amino acids, Curr. Opin. Chem. Biol. 15 (2011) 234–240, https://doi.org/10.1016/j.cbpa.2010.11.009.

[12] M.M. Heberling, B. Wu, S. Bartsch, D.B. Janssen, Priming ammonia lyases and aminomutases for industrial and therapeutic applications, Curr. Opin. Chem. Biol. 17 (2013) 250–260, https://doi.org/10.1016/j.cbpa.2013.02.013.

[13] M. De Villiers, V. Puthan Veetil, H. Raj, J. De Villiers, G.J. Poelarends, Catalytic mechanisms and biocatalytic applications of aspartate and methylaspartate ammonia Lyases, ACS Chem. Biol. 7 (2012) 1618–1628, https://doi.org/10.1021/cb3002792.

[14] P. Müller, C. Fruit, Enantioselective catalytic Aziridinations and asymmetric Nitrene insertions into C−H bonds, Chem. Rev. 103 (2003) 2905–2920, https://doi.org/10.1021/cr020043t.

[15] F. Collet, R.H. Dodd, P. Dauban, Catalytic C–H amination: recent progress and future directions, Chem. Commun. (2009) 5061–5074, https://doi.org/10.1039/B905820F.

[16] Y. Park, Y. Kim, S. Chang, Transition metal-catalyzed C–H amination: Scope, mechanism, and applications, Chem. Rev. 117 (2017) 9247–9301, https://doi.org/10.1021/acs.chemrev.6b00644.

[17] H. Hayashi, T. Uchida, Nitrene transfer reactions for asymmetric C–H amination: Recent Development, Eur. J. Org. Chem. 2020 (2020) 909–916, https://doi.org/10.1002/ejoc.201901562.

[18] Y. Cui, C. He, A silver-catalyzed intramolecular amidation of saturated C–H bonds, Angew. Chem. Int. Ed. 43 (2004) 4210–4212, https://doi.org/10.1002/anie.200454243.

[19] U.T. Bornscheuer, G.W. Huisman, R.J. Kazlauskas, S. Lutz, J.C. Moore, K. Robins, Engineering the third wave of biocatalysis, Nature 485 (2012) 185–194, https://doi.org/10.1038/nature11117.

[20] H. Lu, X.P. Zhang, Catalytic C–H functionalization by metalloporphyrins: recent developments and future directions, Chem. Soc. Rev. 40 (2011) 1899–1909, https://doi.org/10.1039/C0CS00070A.

[21] S. Fantauzzi, A. Caselli, E. Gallo, Nitrene transfer reactions mediated by metallo-porphyrin complexes, Dalton Trans. (2009) 5434–5443, https://doi.org/10.1039/B902929J.

[22] R. Singh, A. Mukherjee, Metalloporphyrin catalyzed C–H amination, ACS Catal. 9 (2019) 3604–3617, https://doi.org/10.1021/acscatal.9b00009.

[23] E.W. Svastits, J.H. Dawson, R. Breslow, S.H. Gellman, Functionalized nitrogen atom transfer catalyzed by cytochrome P-450, J. Am. Chem. Soc. 107 (1985) 6427–6428, https://doi.org/10.1021/ja00308a064.

[24] J.A. McIntosh, P.S. Coelho, C.C. Farwell, Z.J. Wang, J.C. Lewis, T.R. Brown, F. H. Arnold, Enantioselective intramolecular C–H amination catalyzed by engineered cytochrome P450 enzymes in vitro and in vivo, Angew. Chem. Int. Ed. 52 (2013) 9309–9312, https://doi.org/10.1002/anie.201304401.

[25] T.K. Hyster, C.C. Farwell, A.R. Buller, J.A. McIntosh, F.H. Arnold, Enzyme-controlled nitrogen-atom transfer enables regiodivergent C–H amination, J. Am. Chem. Soc. 136 (2014) 15505–15508, https://doi.org/10.1021/ja509308v.

[26] Z.-J. Jia, S. Gao, F.H. Arnold, Enzymatic primary amination of benzylic and allylic C(sp^3)–H bonds, J. Am. Chem. Soc. 142 (2020) 10279–10283, https://doi.org/10.1021/jacs.0c03428.

[27] C.K. Prier, R.K. Zhang, A.R. Buller, S. Brinkmann-Chen, F.H. Arnold, Enantioselective, intermolecular benzylic C–H amination catalysed by an engineered iron-haem enzyme, Nat. Chem. 9 (2017) 629–634, https://doi.org/10.1038/nchem.2783.

[28] C.C. Farwell, R.K. Zhang, J.A. McIntosh, T.K. Hyster, F.H. Arnold, Enantioselective enzyme-catalyzed aziridination enabled by active-site evolution of a cytochrome P450, ACS Cent. Sci. 1 (2015) 89–93, https://doi.org/10.1021/acscentsci.5b00056.

[29] C.C. Farwell, J.A. McIntosh, T.K. Hyster, Z.J. Wang, F.H. Arnold, Enantioselective imidation of sulfides via enzyme-catalyzed intermolecular nitrogen-atom transfer, J. Am. Chem. Soc. 136 (2014) 8766–8771, https://doi.org/10.1021/ja503593n.

[30] E. Alfonzo, D. Hanley, Z.-Q. Li, K.M. Sicinski, S. Gao, F.H. Arnold, Biocatalytic synthesis of α-amino esters via nitrene C–H insertion, J. Am. Chem. Soc. 146 (2024) 27267–27273, https://doi.org/10.1021/jacs.4c09989.

[31] A. Das, S. Gao, R.G. Lal, M.H. Hicks, P.H. Oyala, F.H. Arnold, Reaction discovery using spectroscopic insights from an enzymatic C–H amination intermediate, J. Am. Chem. Soc. 146 (2024) 20556–20562, https://doi.org/10.1021/jacs.4c05761.

[32] R. Singh, M. Bordeaux, R. Fasan, P450-catalyzed intramolecular sp^3 C–H amination with arylsulfonyl azide substrates, ACS Catal. 4 (2014) 546–552, https://doi.org/10.1021/cs400893n.

[33] M. Bordeaux, R. Singh, R. Fasan, Intramolecular C(sp^3)–H amination of arylsulfonyl azides with engineered and artificial myoglobin-based catalysts, Bioorg. Med. Chem. 22 (2014) 5697–5704, https://doi.org/10.1016/j.bmc.2014.05.015.

[34] E.J. Moore, R. Fasan, Effect of proximal ligand substitutions on the carbene and nitrene transferase activity of myoglobin, Tetrahedron 75 (2019) 2357–2363, https://doi.org/10.1016/j.tet.2019.03.009.

[35] S. Roy, D.A. Vargas, P. Ma, A. Sengupta, L. Zhu, K.N. Houk, R. Fasan, Stereoselective construction of β-, γ- and δ-lactam rings via enzymatic C–H amidation, Nat. Catal. 7 (2023) 65–76, https://doi.org/10.1038/s41929-023-01068-2.

[36] J. Majhi, S. Roy, A. Chattopadhyay, R. Fasan, Highly enantioselective construction of Oxazolidinone rings via enzymatic C(sp^3)–H amination, ACS Catal. 15 (2025) 809–816, https://doi.org/10.1021/acscatal.4c06066.

[37] P. Dydio, H.M. Key, H. Hayashi, D.S. Clark, J.F. Hartwig, Chemoselective, enzymatic C–H bond amination catalyzed by a cytochrome P450 containing an Ir(Me)-PIX cofactor, J. Am. Chem. Soc. 139 (2017) 1750–1753, https://doi.org/10.1021/jacs.6b11410.

[38] L. Simkhovich, Z. Gross, Iron(IV) corroles are potent catalysts for aziridination of olefins by chloramine-T, Tetrahedron Lett. 42 (2001) 8089–8092, https://doi.org/10.1016/S0040-4039(01)01717-8.

[39] M.J. Zdilla, M.M. Abu-Omar, Mechanism of catalytic aziridination with manganese Corrole: the often postulated high-valent Mn(V) Imido is not the group transfer reagent, J. Am. Chem. Soc. 128 (2006) 16971–16979, https://doi.org/10.1021/ja0665489.

[40] D.E. Lansky, J.R. Kosack, A.A. Narducci Sarjeant, D.P. Goldberg, An Isolable, Nonreducible high-valent manganese(V) Imido corrolazine complex, Inorg. Chem. 45 (2006) 8477–8479, https://doi.org/10.1021/ic0609251.

[41] T. Hayashi, Y. Morita, E. Mizohata, K. Oohora, J. Ohbayashi, T. Inoue, Y. Hisaeda, Co(II)/co(I) reduction-induced axial histidine-flipping in myoglobin reconstituted with a cobalt tetradehydrocorrin as a methionine synthase model, Chem. Commun. 50 (2014) 12560–12563, https://doi.org/10.1039/C4CC05448B.

[42] K. Oohora, Y. Miyazaki, T. Hayashi, Myoglobin reconstituted with Ni tetradehydrocorrin as a methane-generating model of methyl-coenzyme M reductase, Angew. Chem. Int. Ed. 58 (2019) 13813–13817, https://doi.org/10.1002/anie.201907584.

[43] K. Oohora, H. Meichin, Y. Kihira, H. Sugimoto, Y. Shiro, T. Hayashi, Manganese(V) porphycene complex responsible for inert C–H bond hydroxylation in a myoglobin matrix, J. Am. Chem. Soc. 139 (2017) 18460–18463, https://doi.org/10.1021/jacs.7b11288.

[44] K. Oohora, H. Meichin, L. Zhao, M.W. Wolf, A. Nakayama, J. Hasegawa, N. Lehnert, T. Hayashi, Catalytic cyclopropanation by myoglobin reconstituted with iron porphycene: acceleration of catalysis due to rapid formation of the carbene species, J. Am. Chem. Soc. 139 (2017) 17265–17268, https://doi.org/10.1021/jacs.7b10154.

[45] K. Oohora, Engineered hemoproteins containing non-canonical cofactors toward artificial metalloenzymes, J. Inorg. Biochem. 273 (2025) 113026, https://doi.org/10.1016/j.jinorgbio.2025.113026.

[46] T. Hayashi, Metalloporphycene is an attractive cofactor for hemoproteins, Bull. Chem. Soc. Japan 96 (2023) 1331–1338, https://doi.org/10.1246/bcsj.20230222.

[47] Y. Kagawa, K. Oohora, T. Hayashi, Intramolecular C–H bond amination catalyzed by myoglobin reconstituted with iron porphycene, J. Inorg. Biochem. 252 (2024) 112459, https://doi.org/10.1016/j.jinorgbio.2023.112459.

[48] Y. Kagawa, K. Oohora, T. Himiyama, A. Suzuki, T. Hayashi, Redox engineering of myoglobin by cofactor substitution to enhance cyclopropanation reactivity, Angew. Chem. Int. Ed. 63 (2024) e202403485, https://doi.org/10.1002/anie.202403485.

[49] J.F. Taylor, V.E. Morgan, Oxidation-reduction potentials of the metmyoglobin-myoglobin system, J. Biol. Chem. 144 (1942) 15–20, https://doi.org/10.1016/S0021-9258(18)72551-9.